Journal of Materials Chemistry

Cite this: *J. Mater. Chem.*, 2011, **21**, 12682

www.rsc.org/materials

**PAPER**



# pH-responsive polymeric carrier encapsulated magnetic nanoparticles for cancer targeted imaging and delivery†

**Dongyun Chen,[a] Xuewei Xia,[a] Hongwei Gu,[a] Qingfeng Xu,[a] Jianfeng Ge,[a] Yonggang Li,[b] Najun Li*[a] and Jianmei Lu*[a]**

***Received 21st March 2011, Accepted 9th June 2011***
**DOI: 10.1039/c1jm11195g**

Multifunctional drug delivery systems with favorable compatibility, high selectivity and efficiency are appropriate candidates for future medical applications. For this purpose, a multifunctional nanocomposite that enables selective magnetic resonance imaging and anticancer therapy by encapsulating hydrophobic superparamagnetic nanoparticles and chemotherapeutic agent doxorubicin with a novel biodegradable pH-activated polymeric carrier was synthesized. The as-synthesized amphiphilic polymer has excellent biocompatibility and pH-responsivity. The obtained nanocomposites selectively release the encapsulated drug and magnetic nanoparticles in mildly acidic endosomal/lysosomal compartments due to the degradation of the pH-responsive bonds, resulting in a change of imaging signal and cancer therapy. Furthermore, when compared with the nanocomposites without a targeting moiety, as studied from over-expression of the folic acid receptor tumor cell culturing, the conjugates with folic acid showed a significantly more potent targeting capability.

## Introduction

Currently, studies on the use of multifunctional nanocarriers with diagnosability and therapeutic capacity for biomedical applications are advancing rapidly. These biomedical nanomaterials provide an ideal framework in which active tumor targeting, chemotherapy, imaging or more components can be combined to give multifunctional capabilities. As a diagnostic technique, magnetic resonance imaging (MRI) has proven to be a powerful tool used in clinics. Furthermore, extensive studies over the last decade have already demonstrated that superparamagnetic iron oxide nanoparticles (SPIONPs) with favorable biocompatibility and chemical stability are ideal contrast agents for imaging.[1–3] However, the mono-dispersed nanoparticles synthesized by thermal process are usually stabilized by oleic acid, which do not disperse well in aqueous solution.[4] Consequently, several strategies such as ligand modification and self-assembly have been adopted for enhancing their water solubility and biocompatibility.[5–8] For biomedical applications, the self-assembled nanodrug carriers can be accumulated in tumor cells through the effect of enhanced permeability and retention (EPR).[9,10] These progresses, although valuable, are still affected by the limited functionality and stability of the synthesized polymer-coated magnetic nanoparticles in a physiological medium containing plasma protein and salts. Thus, a multifunctional amphiphilic polymer is required for future developments.

Functional amphiphilic polymers are increasingly used as drug carriers due to their unique load performance,[11–13] where specific guest molecules are encapsulated and released in a controlled manner in response to external specific stimulus such as pH changes (endo- or lysosomes), temperature, enzyme, or redox potential (extra- or intracellular) for cancer diagnosis and therapy.[14–20] In this context, most nano-carriers containing pH-responsive covalent bonds are exploited for intelligent drug delivery. Recently, Lee and co-workers prepared SPIONPs encapsulated pH-responsive polymeric micelles and studied their potential applications in MRI for detecting acidic pathologic areas.[21] Moreover, an amphiphilic polymer modified with cell-specific ligand like folic acid, antibody or sugar, is an attractive approach to successfully target pathologic areas.[22–24] However, the successful ligand modification needs activated groups such as primary amine, alkyne, or activated thiol group on the polymer backbone for subsequent conjugation to biological or synthetic molecules. Reversible addition–fragmentation chain transfer (RAFT) polymerization can easily offer the above functional groups by controlling the polymerization of a large variety of unprotected functional vinyl-based monomers.[25,26] The active tumor targeting moiety can be easily conjugated onto the synthesized amphiphilic copolymers to achieve active target

[a]*Key Laboratory of Organic Synthesis of Jiangsu Province, Key Laboratory of Absorbent Materials and Techniques for Environment, College of Chemistry, Chemical Engineering and Materials Science, Soochow University, Suzhou, China 215123. E-mail: lujm@suda.edu.cn; linajun@suda.edu.cn; Fax: +86 (0) 512-6588 0367; Tel: +86 (0)512-6588 0367*

[b]*Department of Radiology, The First Affiliated Hospital of Soochow University, Soochow University, Suzhou, China 215006*

† Electronic supplementary information (ESI) available: Table S1 and Fig. S1. See DOI: 10.1039/c1jm11195g

delivery. In addition, the RAFT polymerization techniques can even admirably control molecular weight, polydispersity, polymer architecture, placement of reactive groups and solubility in biological environments.[27,28]

In this paper, we report a unique functional diblock polymeric nanocarrier with hydrophobic drug and SPIONP core (Scheme 1). In comparison to our former synthesized random copolymer without a targeting moiety, this process, therefore, is arguably most amenable to controlled delivery or activity in the physiological environment.[29] The functional amphiphilic polymer was synthesized by RAFT polymerization of pH-responsive and water-soluble monomer and successfully conjugated with folic acid (FA) for cancer targeting. The as-synthesized amphiphilic polymer has excellent biocompatibility and pH-responsivity. Doxorubicin (DOX, a widely used anticancer drug), and SPIONPs were simultaneously encapsulated by a polymeric carrier *via* hydrophobic interactions. When specifically recognized and internalized by tumor cells, the pH-responsive polymer shell would release the encapsulated SPIONPs and DOX due to cleavage of acetal moieties in the weakly acidic endosomal/lysosomal compartments, resulting in a change of the MRI signal and drug release, respectively.

## Experimental section

### Materials

Ferric trichloride hexahydrate ($FeCl_3 \cdot 6H_2O$), sodium oleate, sodium methoxide, potassium ferricyanide, *p*-hydroxybenzaldehyde, benzyl chloride, 1-bromododecane, *p*-toluenesulfonic acid (PTSA) and glycerol were all purchased from Shanghai Chemical Reagent Co. Ltd. as analytical regents and used without further purification. 4,4′-Azobis(4-cyanovaleric acid) (V-501) and azobisisobutyronitrile (AIBN) were purchased from Aldrich. *N*-Hydroxysuccinimide (NHS, 99%), *N*-(3-aminopropyl) methacrylamide hydrochloride (APMA), dicyclohexacarbodiimide (DCC, 99%) and 4-dimethylaminopyridine (DMAP, 99%) were purchased from Alfa Aesar. Methacryloyl chloride was produced from Haimen Best Fine Chemical Industry Co. Ltd. and used after distillation. Hydroxyethylacrylate (HEA) was distilled under vacuum and stored at −15 °C under an inert gas atmosphere. Other reagents were commercially available and used as received.

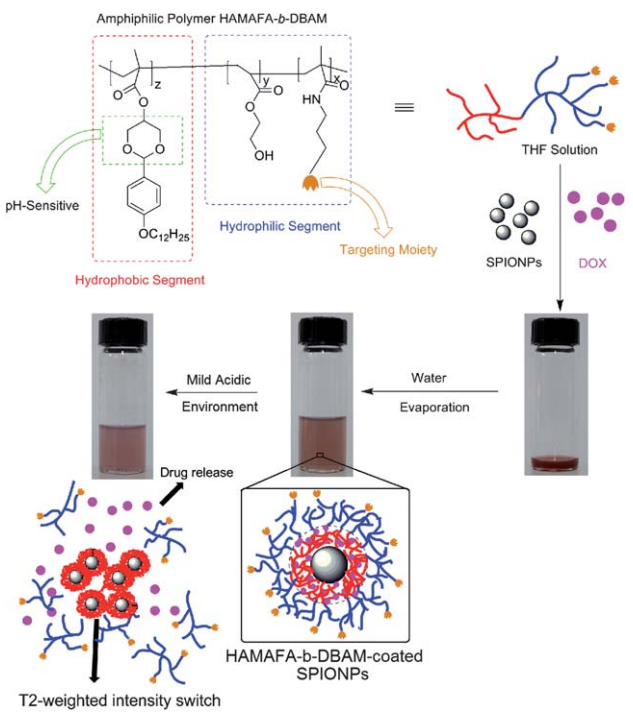


**Scheme 1** Schematic illustration of the synthesis of HAMAFA-*b*-DBAM-coated SPIONPs for targeted imaging and delivery.

### Synthesis of RAFT agent 4-cyanopentanoic acid dithiobenzoate (CAD)

CAD was synthesized according to the literature with some modifications.[30] Briefly, 12.8 g of benzyl chloride was added dropwise to a sodium methoxide methanol solution (172 g, 12.6 wt%) containing 12.8 g of elemental sulfur. Subsequently, the obtained mixture was refluxed for 10 h under inert atmosphere. The crude sodium dithiobenzoate solution was extracted by diethyl ether, 1.0 M hydrochloric acid and sodium hydroxide aqueous solution, respectively and finally yielded a solution of sodium dithiobenzoate. Potassium ferricyanide solution (500 mL, 6.5 wt%) was added dropwise to the sodium dithiobenzoate over a period of 1 h with vigorous stirring. The obtained red precipitate was filtered, washed with deionized water, and dried in vacuum at room temperature overnight. Dithiobenzoyl disulfide (8.50 g, 0.28 mol) was added slowly to the distilled ethyl acetate (150.0 mL) solution containing 11.68 g of V-501 (0.42 mol). After refluxing for 18 h, the reaction solution was concentrated in vacuum and isolated by column chromatography (ethyl acetate–hexane, 2 : 3). Anal. Calcd. for $C_{13}H_{13}NO_2S_2$: C 55.89%, H 4.69%, N 5.01%, S 22.95%. Found: C 55.76%, H 4.48%, N 5.08%, S 23.00%. $^1$H NMR (400 MHz, $CDCl_3$), $\delta$ (ppm): 7.91 (d, $J$ = 7.59 Hz, 2H, $C_6H_4$), 7.58 (t, $J$ = 7.47 Hz, 1H, $C_6H_4$), 7.41 (t, $J$ = 7.79 Hz, 2H, $C_6H_4$), 2.75 (m, 2H, $CCH_2$), 2.45 (m, 2H, $\underline{CH_2}COOH$), 1.95 (s, 3H, $CH_3$).

### Synthesis of 4-*n*-dodecyloxybenzalacetal monomer (DBAM)

4-*n*-Dodecyloxybenzaldehyde (DBD) was synthesized according to the literature with some modifications.[31] Typically, 1-bromododecane (29.9 g, 120 mmol) was added dropwise to an acetone (150 mL) solution containing anhydrous potassium carbonate (20.7 g, 150 mmol) and *p*-hydroxybenzaldehyde (12.2 g, 100 mmol). After heating under reflux with stirring for 14 h, the crude product was purified by column chromatography (ethyl acetate–petroleum ether 60–90°C, 1 : 10).

After that, DBD (8.7 g, 30 mmol) reacted with glycerol (2.76 g, 30 mmol) in 50 mL toluene using PTSA (0.5 g) as the catalyst. The solution was refluxed for 14 h and the water formed by dehydrogenation reaction was removed by the oil–water separator. Then, the mixture was concentrated and washed with potassium carbonate solution (1%, 80 mL) to remove the acid catalyst and any remaining glycerol. After that, the precipitate was collected and purified by column chromatography (ethyl acetate–petroleum ether, 1 : 2) to obtain 4-*n*-dodecyloxybenzalacetal (DBA).

Methacryloyl chloride (2.3 g, 22 mmol) was added slowly to the anhydrous tetrahydrofuran (20 mL) solution containing triethylamine (4.5 g, 44 mmol) and DBA (4.0 g, 11 mmol) and cooled to 0 °C in a water–ice bath. After constantly stirring for another 12 h at room temperature, the mixture was filtered off to remove the byproduct. The obtained filtrate was concentrated and purified by column chromatography (ethyl acetate–petroleum ether, 1 : 8). Anal. Calcd. for $C_{26}H_{40}O_5$: C 72.19%, H 9.32%, O 18.49%. Found: C 72.30%, H 9.28%, O 18.42%. $^1$H NMR (400 MHz, $CDCl_3$), $\delta$ (ppm): 7.41 (d, $J$ = 8.39 Hz, 2H, $C_6H_4$), 6.89 (d, $J$ = 8.41 Hz, 2H, $C_6H_4$), 6.30 (s, 1H, $CCH_2$), 5.65 (s, 1H, $CCH_2$), 5.52 (s, 1H, $C_6H_4\underline{CH}$), 4.75 (s, 1H, CHO), 4.31 (d, $J$ = 12.88 Hz, 2H, $CH\underline{CH_2}O$), 4.18 (d, $J$ = 12.92 Hz, 2H, $CH\underline{CH_2}O$), 3.95 (t, $J$ = 6.59 Hz, 2H, $C_6H_4O\underline{CH_2}$), 2.01 (s, 3H, $CH_3$), 1.81–1.72 (m, 2H, $\underline{CH_2}CH_2O$), 1.49–1.38 (m, 2H, $\underline{CH_2}CH_2CH_2O$), 1.26 (m, 16H, $CH_2$), 0.88 (t, $J$ = 6.68 Hz, 3H, $CH_2\underline{CH_3}$). $^{13}$C NMR (75 MHz, $CDCl_3$), $\delta$ (ppm): 167.45 (s, 1C, COO), 159.95 (s, 1C, C), 136.28 (s, 1C, $\underline{C}CH_3$), 132.25 (s, 1C, C), 127.57 (s, 2C, CH), 126.50 (s, 1C, $C\underline{CH_2}$), 114.52 (s, 2C, CH), 74.21 (s, 1C, $CH_2\underline{C}O$), 69.25 (s, 2C, $\underline{CH_2}CO$), 68.28 (s, 1C, $CH\underline{CH_2}O$), 32.16 (s, 1C, $\underline{CH_2}CH_2CH_3$), 29.28–29.88 (m, 7C, $CH_2$), 26.24 (s, 1C, $\underline{CH_2}CH_2CH_2O$), 22.94 (s, 1C, $\underline{CH_2}CH_3$), 18.52 (s, 1C, $C\underline{CH_3}$), 14.39 (s, 1C, $CH_3$).

### Synthesis of HAMA-*b*-DBAM

HAMA was prepared by RAFT polymerization of HEA and APMA using CAD as a transfer agent. Typically, 5.3 mg (0.02 mmol) CAD was added to the aqueous solution containing 2.5 mg of V-501, 1.22 g of HEA (10.5 mmol) and 268 mg of APMA (1.5 mmol). Then, the tube was sealed and cycled between vacuum and nitrogen for three times. After 5 h reaction in oil bath at 70 °C, the mixture was concentrated and washed with a large amount of acetone. The obtained copolymer was dried under vacuum and stored in a desiccator for further polymerization.

The amphiphilic diblock polymer HAMA-*b*-DBAM was synthesized using HAMA macrochain transfer agent. In a typical polymerization procedure, 1.2 g of HAMA was added to a dimethylsulfoxide solution containing 3 mg AIBN and 200 mg (0.31 mmol) DBAM and then placed in an oil bath at 70 °C for 5 h. The mixture was concentrated and washed with a large amount of ethyl ether. After washing, the obtained diblock polymer was dried under vacuum overnight and stored in a desiccator.

### Synthesis of folate conjugated diblock polymer HAMAFA-*b*-DBAM

Conjugation procedure was achieved according to the literature reported elsewhere.[11,32,33] First, thiocarbonylthio end group of HAMA-*b*-DBAM was removed according to the literature with some modifications. Briefly, 500 mg of HAMA-*b*-DBAM was dissolved in 10 mL *N*,*N*-dimethylformamide (DMF) containing 30 mg of AIBN. The DMF solution was sealed and cycled between vacuum and nitrogen for three times. After stirring at 70 °C for 5 h, the mixture was precipitated in anhydrous ether. The obtained diblock polymer was dried under vacuum and stored in a desiccator for further use. Second, folate NHS ester was prepared by the following procedure: 0.62 g of DCC and 0.51 g NHS were added to dry dimethylformamide (50 mL) solution containing 2.0 g of folic acid for 12 h at room temperature in the dark. The solution was filtered off and precipitated in diethyl ether. The obtained yellow powder was washed several times with anhydrous ether and used immediately for the next step. Then, FA-NHS (30 mg) was added to dry pyridine containing 100 mg of the above polymer. The solution was shaken for 12 h at room temperature and the mixture was precipitated in 40% acetone in diethyl ether. The filtrate was concentrated and stored in the dark at 4 °C. The $^1$H NMR spectrum showed nearly 100% conjugation of FA. $^1$H NMR (400 MHz, DMSO-$d_6$), $\delta$ (ppm): 8.63–6.62 (folic acid and $CH_2\underline{NH_2}$), 4.21–3.76 ($COOCH_2CH_2$ and $CH_2OH$), 2.85 ($NH\underline{CH_2}$ and $\underline{CH_2}NH_2$), 1.21 ($CH_3$).

### Synthesis of superparamagnetic iron oxide nanoparticles (SPIONPs)

SPIONPs were synthesized according to the literature with some modifications.[34] Briefly, 9.1 g (30 mmol) sodium oleate and 2.7 g (10 mmol) of $FeCl_3\cdot 6H_2O$ were dissolved in a solvent mixture composed of 20 mL ethanol, 15 mL water and 35 mL hexane. After heating at 70 °C for 4 h, the organic layer was washed and evaporated to obtain iron–oleate complex. Then, 9.0 g (10 mmol) of the iron–oleate complex and 1.4 g of oleic acid (5 mmol) were dissolved in 50 g of trioctylamine at room temperature. The mixture was heated at 320 °C for 30 min and then cooled to room temperature. The black iron oxide magnetic nanoparticles were washed several times with ethanol and dried at 60 °C for 24 h.

### Synthesis of HAMAFA-*b*-DBAM-coated SPIONPs

Oleic acid-stabilized SIONPs (2 mg) and HAMAFA-*b*-DBAM (5 mg) were dissolved in tetrahydrofuran (1 mL). Then, 5 mL of distilled water was added to the above solution with vigorous shaking and the resulting colloid was stirred vigorously for 24 h to evaporate tetrahydrofuran. After that, the colloid was separated by centrifugation and the obtained HAMAFA-*b*-DBAM-coated SPIONPs were washed three times with distilled water to remove the unbound copolymer (yield: 76%). In addition, the encapsulation % of SPIONPs is 73% (confirmed by inductively coupled plasma atomic emission spectroscopy, ICP-AES).

The critical micelle concentration (CMC) of the diblock copolymer was determined by a fluorescence technique using pyrene as a fluorescence probe. The concentration of pyrene was fixed at 0.6 μM and the concentration of the polymer was varied from 0.5 μg $mL^{-1}$ to 0.2 mg $mL^{-1}$. The CMC was determined from the crossover point in the low concentration range. The CMC of the diblock copolymer was 9.3 mg $L^{-1}$, which is not only strong evidence to the formation of nanoparticles but also an important parameter in evaluating the stability of the nanoparticles in the blood post administration.

### Drug loading and release

To evaluate the drug loading and release properties, doxorubicin (DOX) was used as a model anticancer agent. Free water-insoluble DOX was extracted from doxorubicin hydrochloride (DOX·HCl) according to the procedure reported previously.[35]

 

The DOX solution (5 mg $mL^{-1}$) was added to 0.8 mL of the above HAMAFA-*b*-DBAM–SPIONPs solution in tetrahydrofuran, followed by slow addition of 10 mL phosphate buffer (20 mmol $mL^{-1}$, pH = 7.4). And the solution was shaken for 24 h to allow partitioning of the DOX into the nanoparticles. Then, the drug loaded core–shell magnetic nanoparticles were separated from free DOX solution using a magnet. The concentration of the remaining DOX solution was determined using a fluorescence spectrophotometer at $\lambda_{ex}$ = 475 nm and $\lambda_{em}$ = 592 nm, respectively. To confirm the amount of drug stored by the nanoparticles, a standard plot was prepared under identical conditions.

The drug release test was performed by suspending the DOX-loaded nanoparticles in phosphate buffered saline (PBS) (pH = 7.4) with shaking in a water bath maintaining the temperature at 37 °C. To determine the release amount at any given time, 1.0 mL of the solution was withdrawn after centrifugation and the same volume of PBS was added to keep the volume constant. To determine the release amount at any given pH value, the obtained colloid was adjusted to different pH values by using acetate buffer. Drug concentration of the withdrawn solution was analyzed by measuring the UV absorbance at 485 nm, respectively. The experiments were conducted in triplicate and the results are average data with standard deviations.

### Cell culture and preparation

Hepatoma 7402 (FR−) and human KB (FR+) cell lines (purchased from Shanghai Cell Institute Country Cell Bank, China) were cultured as monolayer in RPMI-1640 medium supplemented with 10% heat-inactivated fetal bovine serum at 37 °C in a humidified incubator (5% $CO_2$ in air, v/v).

### *In vitro* cytotoxicity

Sulforhodamine B (SRB) is used as an assay for assessing the effects of drug carriers in various concentrations.[36] In brief, hepatoma 7402 or KB cells were seeded in 96-well plates ($1.3 \times 10^4$ cells per well) and four duplicate wells were set up in each sample. The culture medium was replaced with the medium containing different concentrations of DOX-free HAMAFA-*b*-DBAM-coated SPIONPs (0, 0.391, 0.781, 1.563, 3.125, 6.25, 12.5, 25, 50 and 100 μg $mL^{-1}$) or DOX-loaded nanocomposites (HAMA-*b*-DBAM-coated SPIONPs, or HAMAFA-*b*-DBAM-coated SPIONPs, or free DOX at different DOX concentrations) and cultured at 37 °C in a humidified incubator (5% $CO_2$ in air, v/v). After culturing for 72 h, the medium was poured away and 10% (w/v) trichloroacetic acid in Hank's balanced salt solution (100 μL) was added and stored at 4 °C for 1 h. Then, the stationary liquid was discarded, the cells were washed with deionized water for five times before air drying and stained with 0.4% (w/v) SRB solution (100 μL per well) for 30 min at room temperature. Following the removal of SRB, the cells were washed with 0.1% acetic acid solution for five times. The bound SRB dye was solubilized with 10 mmol $L^{-1}$ Tris–base solution (150 μL, pH = 10.5). The test optical density (OD) value was calculated by the absorbance at 531 nm of each individual well measured with a spectrophotometer.

### Cellular uptake of DOX

Human KB cells and Hepatoma 7402 cells were seeded in 96-well plates ($1.3 \times 10^4$ cells per well) and incubated overnight at 37 °C in a humidified incubator. The dispersion was prepared in RPMI-1640 medium as described above. The concentrations of the HAMAFA-*b*-DBAM-coated SPIONPs and HAMA-*b*-DBAM-coated SPIONPs were 10 μg $mL^{-1}$. Cells were cultured with the above solution for 30 min and 3 h and observed using fluorescence microscopy. In addition, the culture media were removed and the cells were washed three times with PBS prior to fluorescence observation. The fluorescence images were acquired using an Olympus IX-51 inverted microscope equipped with 100 W mercury–xenon arc lamp excitation light source and high speed CCD camera.

### Flow cytometry

Hepatoma 7402 and human KB cells were cultured as monolayer in RPMI-1640 medium supplemented with 10% heat-inactivated fetal bovine serum. The medium was then replaced with a freshly prepared medium containing DOX-loaded HAMA-*b*-DBAM-coated SPIONPs (FA-free) and HAMAFA-*b*-DBAM-coated SPIONPs (FA-conjugated) with an equivalent DOX concentration of 10 μg $mL^{-1}$. The cells were incubated for the desired time. After that, the suspensions were centrifuged and washed three times with cold PBS, and then resuspended in PBS. Flow cytometry was performed on a BD FACS Calibur.

### MRI experiments

MRI experiments were carried out with a 0.5 tesla (T) superconducting unit (GE Vectra, International General Electric, Slough, UK). HAMAFA-*b*-DBAM-coated SPIONPs were loaded into eppendorf tubes for imaging. Multisection $T_2$-weighted fast spin-echo sequences were performed in at least two orthogonal planes to obtain MR phantom images. MRI signal intensity was calculated using the in-built software.

### Characterization methods

TEM images were obtained using a TecnaiG220 electron microscope at an acceleration voltage of 200 kV. Number-average molecular weight ($M_n$), weight-average molecular weight ($M_w$) and polydispersity index (PDI) were measured by gel permeation chromatography (GPC) utilizing waters 1515 pump. Monomer conversion was determined by gravimetry. $^1H$ NMR and $^{13}C$ NMR were measured by INOVA 400 MHz NMR instrument. Emission and excitation spectra were obtained using Edinburgh-920 fluorescence spectra photometer. UV-Vis absorption spectra were recorded by a Perkin-Elmer Lambda-17 spectrophotometer.

## Results and discussion

### Synthesis and characterization of HAMAFA-*b*-DBAM

The synthetic process of HAMAFA-*b*-DBAM is shown in Scheme 1. Four diblock copolymers with different $M_w$ and PDI were synthesized by varying the mole ratio of the macro-chain transfer agent HAMA and the monomer. The molecular weights

and PDIs of HAMA before and after block polymerization were measured by GPC. Based on an evaluation of the characterization data of the diblock copolymers, HAMAFA-*b*-DBAM polymerized with a monomer feed ratio of 10 : 1 was chosen for further investigation (Table S1†). As shown in Fig. 1a, both of the elution peaks are relatively mono-modal and symmetric and without any shoulder or evident tailing at the lower or higher molecular weight side. In addition, a clear shift (from A to B) toward the direction of higher molecular weight is observed, confirming the complete consumption of the macro-chain transfer agent and successful block copolymer formation.[37,38]

Moreover, to enhance the specific targeting capability of the block copolymer, folic acid was conjugated. In consideration of the aminolysis of the pendant primary amine groups, the ω-thiocarbonylthio functionality was removed by addition of excess AIBN. The successful removal of ω-thiocarbonylthio functionality and conjugation of FA were confirmed by a UV-Vis detector as shown in Fig. 1b. Obvious characteristic absorption peak changes are observed, which demonstrate the successful thiocarbonylthio removal and FA conjugation processes.[11]

## Synthesis and characterization of HAMAFA-*b*-DBAM-coated SPIONPs

Generally, an amphiphilic polymer which forms micelles in water *via* self-assembly can encapsulate the hydrophobic guest molecules. In our approach, the hydrophobic long alkyl side chain of DBAM can insert into the oleic acid shell of SPIONPs with the hydrophilic part on the surface to form water soluble nanocomposites. Scheme 2 shows photographs of the SPIONPs

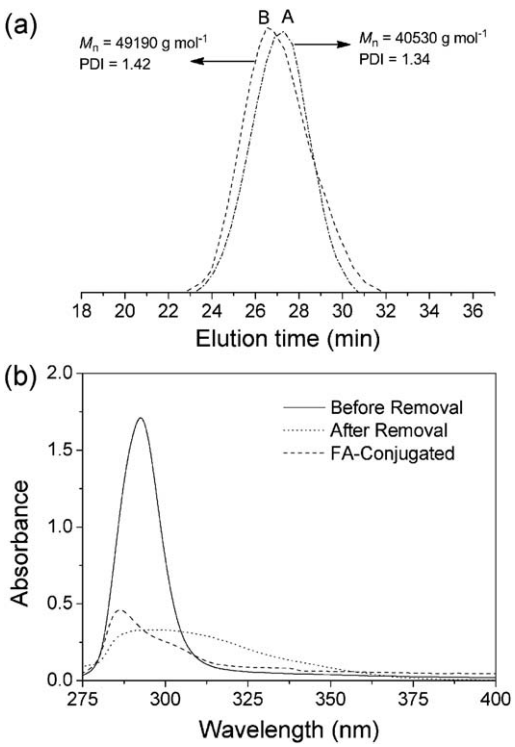


**Fig. 1** (a) GPC curves of HAMA (A) and HAMAFA-*b*-DBAM (B); (b) UV-Vis spectra of HAMA-*b*-DBAM, HAMA-*b*-DBAM after thiocarbonylthio removal and HAMAFA-*b*-DBAM.

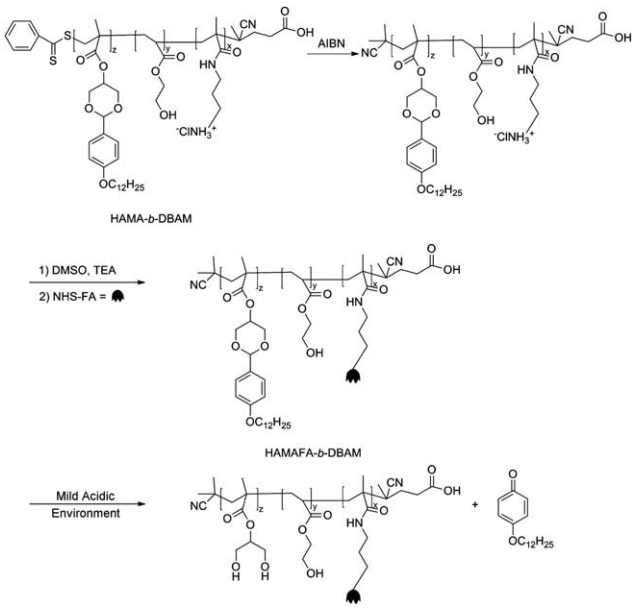


**Scheme 2** Schematic illustration of the synthesis of HAMAFA-*b*-DBAM.

before and after assembling with HAMAFA-*b*-DBAM and in mildly acidic condition. Upon self-assembly with amphiphilic polymer, the oleic acid-capped SPIONPs, which initially dispersed in tetrahydrofuran, transferred into water to form a homogeneous aqueous solution. This water soluble nanocomposite was stable in neutral aqueous solution and is suitable for further usage in biomedical applications. However, after acidification under acidic conditions for several minutes, the colloidal solution became cloudy and even precipitation occurred at the bottom of the vial, implying an increased aggregation of the hydrophobic SPIONPs.

To evaluate the pH-response behavior of the nanocomposites in aqueous solution, TEM images of the as-synthesized nanocomposites in solutions of different pH were taken. As shown in Fig. 2a, the nanocomposites are uniformly distributed and gradually aggregate under a mildly acidic environment, while the colloid is well dispersed in a neutral environment. This agglomeration probably attributed to the release of hydrophobic SPIONPs from the carrier into a hydrophilic environment. Size distribution of the nanocomposite dispersed in water was studied using DLS to further confirm the result. As shown in Fig. 2b, the respective intensity-average hydrodynamic diameters are about 20 nm and 1800 nm before and after acidification. Similar to the results from TEM images, the hydrodynamic diameter of the nanocomposites increases with decreasing pH. Hence, these nanocomposites are adequate for selective anti-tumor drug delivery.

## Evaluation of drug loading and release

The amount of DOX encapsulated by nanocomposites was determined by comparing the absorbed DOX solution with the standard plot, using a fluorescence spectrophotometry at $\lambda_{ex}$ = 475 nm and $\lambda_{em}$ = 592 nm, respectively. DOX loading in the formulation was 78 ± 4 μg of drug per mg of nanocomposite.

 

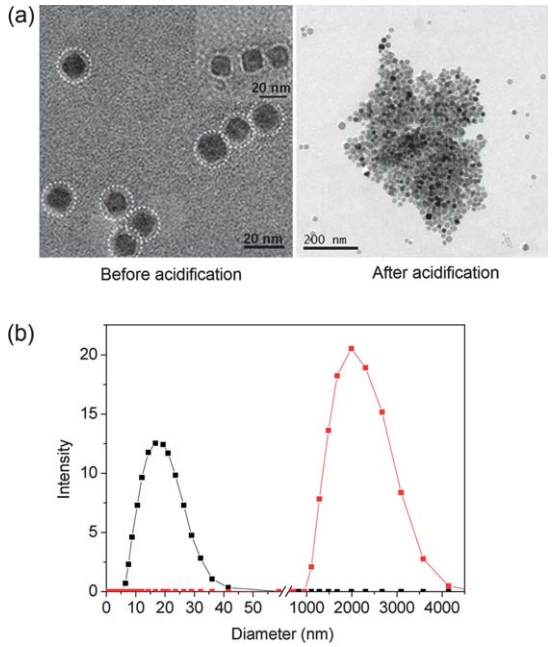


**Fig. 2** TEM images (a) and DLS diagram (b) of HAMAFA-*b*-DBAM-coated SPIONPs before and after acidification.

The nanocomposites encapsulated DOX efficiently (a loading efficiency of about 79%), which was sufficient to be injected to kill cancer cells.

To evaluate the drug release behavior, the *in vitro* cumulative DOX release profiles of the nanocomposite were investigated at 37 °C and at two different pH values (pH 7.4 and 5.0) as shown in Fig. 3a. The release studies showed that under neutral pH condition (pH = 7.4), minimal DOX release (<5%) was observed within 12 h, implying that the nanocomposites were relatively stable under a neutral environment. This good stability may be because of the interactions between the hydrophobic DOX and long hydrophobic alkyl chain of the polymer and SPIONPs. However, in a weakly acidic environment (pH = 5.0), a much faster release rate of DOX was observed. Cumulative DOX release for 12 h at 37 °C was about 92% of the loaded drug. This clearly shows that the nanocomposites can encapsulate hydrophobic drugs for selective release in a slightly acidic environment. Fig. 3b shows the hydrolysis profiles of HAMAFA-*b*-DBAM at pH 5.0 and 7.4, which were determined by $^{1}$H NMR peak integrals *versus* time. These results revealed that the hydrolysis degree is highly pH dependent, in agreement with the findings from the drug release profiles. This outstanding pH-responsive behavior is highly desirable for selective drug delivery because it can obviously prevent the premature release during the circulation in the physiological environment, thus ensuring a sufficient drug release to effectively kill tumor cells.

### Evaluation of cytotoxicity and drug uptake

The sulforhodamine B (SRB) assay is used to assess the cytotoxicity of the nanocomposite. As shown in Fig. 4a, the cells incubated in the nanocomposite for 72 h displayed high cell viability (>83%). No significant cytotoxicity was observed even at a high concentration. The toxicological effects may be ascribed

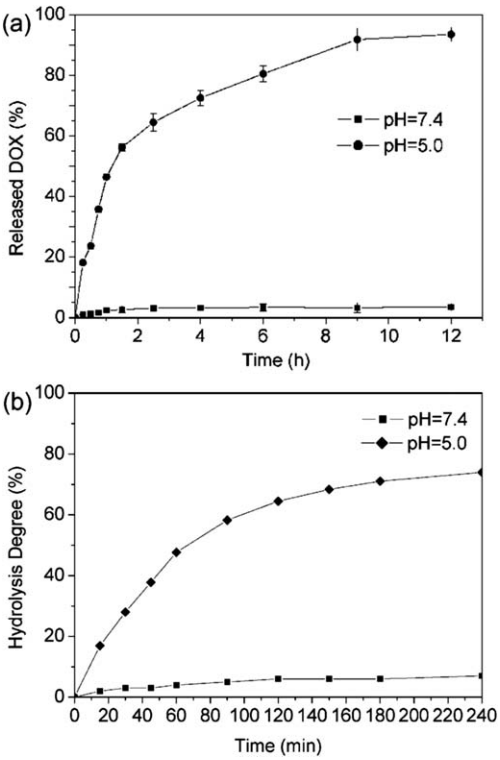


**Fig. 3** (a) Release of doxorubicin *in vitro* from drug-loaded HAMAFA-*b*-DBAM-coated SPIONPs; (b) hydrolysis degree of HAMAFA-*b*-DBAM as a function of time at different pH at 37 °C.

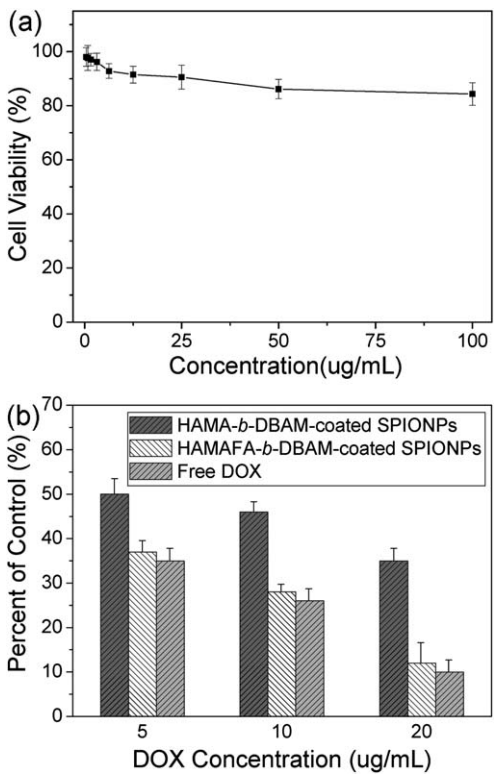


**Fig. 4** *In vitro* cell viability of (a) DOX-free HAMAFA-*b*-DBAM-coated SPIONPs and (b) DOX-loaded nanocomposites (HAMA-*b*-DBAM-coated SPIONPs, HAMAFA-*b*-DBAM-coated SPIONPs and free DOX) at different DOX concentrations.

to the biocompatible and nontoxic nature of the polymer shell. The excellent biocompatibility indicates that the nanocomposite might be safe for further biomedical applications. To further determine the effectiveness of the nanocomposites mediating cytotoxicity against KB cells, DOX-loaded nanocomposites and free DOX at different DOX concentrations were incubated with cells. As shown in Fig. 4b, in all DOX concentrations, both free DOX and DOX-loaded HAMAFA-*b*-DBAM-coated SPIONPs showed nearly the same level of cytotoxicity, which was at least 15% greater than that of the DOX-loaded HAMA-*b*-DBAM-coated SPIONPs. The obvious differences in cytotoxicity demonstrate that the FA-conjugation highly increases the cellular uptake, thus bringing about cytotoxicity increase of the nanocomposites.

Moreover, *in vitro* experiments were used to demonstrate the selective release and targeting properties of the nanocomposites. Since DOX itself is a fluorophore, the fluorescence intensity can be used to evaluate the specific intracellular activity of the nanocomposites in a folate receptor positive (KB cells) and negative (7402) cancer cell line. The KB cell uptake and intracellular distribution of the nanocomposites with (HAMAFA-*b*-DBAM-coated SPIONPs) and without (HAMA-*b*-DBAM-coated SPIONPs) FA groups for 0.5 and 3 h were studied by fluorescence microscopy as shown in Fig. 5a. In addition, by way of contrast, fluorescence images of 7402 cells incubated with HAMAFA-*b*-DBAM-coated SPIONPs are shown in Fig. S1†.

After incubation for 0.5 h, no obvious differences in the fluorescence intensity were observed between the two nanocomposites. They were both uptaken by the KB cells through the simple endocytosis process. With an incubation of 3 h, the fluorescence intensity of the FA-conjugated nanocomposites was much stronger compared to that without FA conjugation and FA-conjugated nanocomposites incubated with receptor negative cancer cell, implying the cellular internalization enhancement associated with the targeting capacity of the FA group *via* the folate receptor-mediated endocytosis.[39–42] Moreover, this difference demonstrates that the targeting moiety offered by folic acid is efficient at enhancing the tumor cell targeting *in vitro*, which corroborates the findings from the SRB measurements. The mean fluorescence intensity on FR+ and FR− cells with DOX-loaded HAMA-*b*-DBAM-coated SPIONPs and HAMAFA-*b*-DBAM-coated SPIONPs was further confirmed by flow cytometry. As shown in Fig. 5b, it is remarkable to note that the FR+ cells incubated with HAMAFA-*b*-DBAM-coated SPIONPs for 3 h exhibited higher cellular uptake when compared with the other incubations. This demonstrates the sustained release of anti-tumor drugs from the carrier due to the pH-dependent degradation property of the nanocomposites. These results show that successful folic acid modification to the diblock copolymer shell can increase the nanocomposites uptake and hence, guarantee more drugs delivered to the tumor sites but not to the non-cancerous fibroblasts.

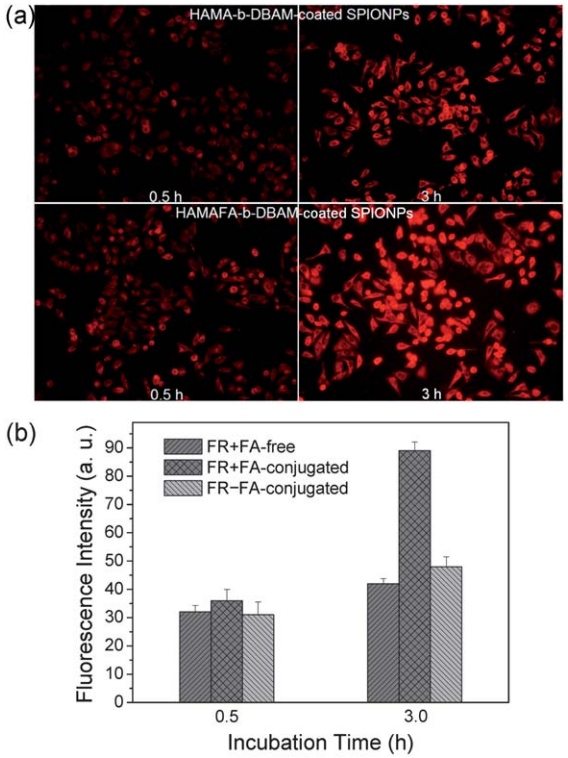


**Fig. 5** (a) Fluorescence images of FR+ cells incubated with HAMA-*b*-DBAM-coated SPIONPs and HAMAFA-*b*-DBAM-coated SPIONPs for 0.5 h and 3 h. (b) Mean fluorescence intensity on FR+ and FR− cells with DOX-loaded (10 μg $mL^{-1}$) HAMA-*b*-DBAM-coated SPIONPs (FA-free) and HAMAFA-*b*-DBAM-coated SPIONPs (FA-conjugated) in solution at different incubation times. (*e.g.* FR + FA-free means DOX-loaded HAMA-*b*-DBAM-coated SPIONP nanocomposites incubated with KB cells.)

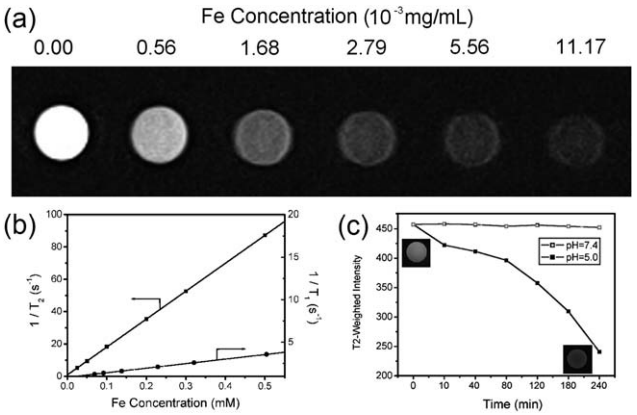


**Fig. 6** (a) $T_2$-weighted MR images and (b) relaxation rates ($1/T_1$ and $1/T_2$) of the aqueous dispersion of HAMAFA-*b*-DBAM-coated SPIONPs at various Fe concentrations. (c) Time-course of mean $T_2$-weighted intensity of HAMAFA-*b*-DBAM-coated SPIONPs in solutions with different pH.

### *In vitro* MRI experiments

In view of the low cytotoxicity and high colloidal stability, the nanocomposite may be a safe MRI contrast agent *in vivo*. Fig. 6a shows the $T_2$-weighted images of the nanocomposites suspended in water at various Fe concentrations. As can be seen, the pure water as control shows a bright white $T_2$-weighted MR image because of the water protons' spin relaxation. After that, the MR signal increases with decreasing content of

 

HAMAFA-*b*-DBAM-coated SPIONPs, confirming the capability of the SPIONP core in enhancing the transverse proton relaxation process. Fig. 6b shows the relaxation rate, the specific relaxivities are 4.9 and 163 $mM^{-1}$ $s^{-1}$ for $r_1$ and $r_2$, respectively. The relaxivity of $r_2/r_1$ is an important aspect to evaluate the efficiency of $T_2$-contrast agent. In our approach, $r_2/r_1$ is calculated to be 33, which is much larger than that of dextran-coated SPIONPs.[43]

To further evaluate the degradation influence to the nanocomposites, magnetic resonance phantom imaging was used. The intensity of the colloid showed a significant $T_2$-weighted intensity drop-off in an acidic environment (pH = 5.0) in comparison to the control ([Fe] = $8.38 \times 10^{-4}$ mg $mL^{-1}$), which exhibited high sensitivity and rapid detectability by MRI. The $T_2$-weighted images of the nanocomposites before and after acidification are shown in Fig. 6c and the $T_2$-weighted intensity was calculated using a built-in software. In addition, about 52% of the $T_2$ intensity decrease was observed after acidification for 4 h, consistent with the above assumptions. The decrease in $T_2$-weighted intensity is probably attributed to the partial aggregation of hydrophobic SPIONPs. In acidic condition, the drug is released and then the hydrophobic SPIONPs aggregate resulting in MR sensitivity increase.[44–46] In addition, MR imaging was further used to confirm the targetability of HAMAFA-*b*-DBAM-coated SPIONPs. The $T_2$-weighted MR image (Fig. S5†) of KB cells incubated with HAMAFA-*b*-DBAM-coated SPIONPs showed an obvious negative contrast enhancement in comparison to the HAMA-*b*-DBAM-coated SPIONPs, which revealed effective nanocomposites internalization inside the KB cells.

## Conclusions

In conclusion, by encapsulating hydrophobic superparamagnetic nanoparticles and chemotherapeutic agent doxorubicin with a biodegradable pH-activated polymeric carrier, we can construct a multifunctional nanocomposite that enables selective magnetic resonance imaging and anticancer therapy. Folic acid was also conjugated on the polymeric carrier as the targeting moiety. The obtained biocompatible and water-stable HAMAFA-*b*-DBAM-coated SPIONP colloids can directionally image and release in a mildly acidic pathological site *via* a degradation and aggregation process, which can provide a promising potential application for early detection and therapy of some cancers.

## Acknowledgements

This work was supported by the National Natural Science Foundation of China (Grant Nos. 20876101, 20902065, 21071105 and 21076134), the Natural Science Foundation of the Jiangsu Higher Education Institutions of China (Grant No.09KJB430010) and Innovative Research Team of Advanced Chemical and Biological Materials, Suzhou University.

## Notes and references

1 J. Gao, H. Gu and B. Xu, *Acc. Chem. Res.*, 2009, **42**, 1097.
2 C. Sun, J. S. H. Lee and M. Zhang, *Adv. Drug Delivery Rev.*, 2008, **60**, 1252.
3 H. Lee, E. Lee, N. K. Jang, Y. Y. Jeong and S. Jon, *J. Am. Chem. Soc.*, 2006, **128**, 7383.
4 J. Park, M. K. Yu, Y. Y. Jeong, J. W. Kim, K. Lee, V. N. Phan and S. Jon, *J. Mater. Chem.*, 2009, **19**, 6412.
5 X. Michalet, F. F. Pinaud, L. A. Bentolila, J. M. Tsay, S. Doose, J. J. Li, G. Sundaresan, A. M. Wu, S. S. Gambhir and S. Weiss, *Science*, 2005, **307**, 538.
6 N. Pradhan, D. M. Battaglia, Y. Liu and X. Peng, *Nano Lett.*, 2007, **7**, 312.
7 J. Qin, Y. S. Jo and M. Muhammed, *Angew. Chem., Int. Ed.*, 2009, **48**, 7845.
8 R. Hao, R. Xing, Z. Xu, Y. Hou, S. Gao and S. Sun, *Adv. Mater.*, 2010, **22**, 2729.
9 M. Zhao, D. A. Beauregard, L. Loizou, B. Davletov and K. M. Brindle, *Nat. Med. (N. Y.)*, 2001, **7**, 1244.
10 S. Laurent, D. Forge, M. Port, A. Roch, C. Robic, E. L. Vander and R. N. Muller, *Chem. Rev.*, 2008, **108**, 2064.
11 N. Nasongkla, E. Bey, J. Ren, H. Ai, C. Khemtong, J. S. Guthi, S. F. Chin, A. D. Sherry, D. A. Boothman and J. Gao, *Nano Lett.*, 2006, **6**, 2427.
12 V. P. Torchilin, *Adv. Drug Delivery Rev.*, 2006, **58**, 1532.
13 H. Kawaguchi, *Prog. Polym. Sci.*, 2000, **25**, 1171.
14 R. M. Sawant, J. P. Hurley, S. Salmaso, A. Kale, E. Tolcheva, T. S. Levchenko and V. P. Torchilin, *Bioconjugate Chem.*, 2006, **17**, 943.
15 D. Schmaljohann, *Adv. Drug Delivery Rev.*, 2006, **58**, 1655.
16 A. K. Bajpai, S. K. Shukla, S. Bhanu and S. Kankane, *Prog. Polym. Sci.*, 2008, **33**, 1088.
17 S. Ganta, H. Devalapally, A. Shahiwala and M. Amiji, *J. Controlled Release*, 2008, **126**, 187.
18 L. Linderoth, G. H. Peters, R. Madsen and T. L. Andresen, *Angew. Chem., Int. Ed.*, 2009, **121**, 1855.
19 H. Koo, H. Lee, S. Lee, K. H. Min, M. S. Kim, D. S. Lee, Y. Choi, I. C. Kwon, K. Kim and S. Y. Jeong, *Chem. Commun.*, 2010, **46**, 5668.
20 J. Y. Ko, S. Park, H. Lee, H. Koo, M. S. Kim, K. Choi, I. C. Kwon, S. Y. Jeong, K. Kim and D. S. Lee, *Small*, 2010, **6**, 2539.
21 G. H. Gao, G. H. Im, M. S. Kim, J. W. Lee, J. Yang, H. Jeon, J. H. Lee and D. S. Lee, *Small*, 2010, **6**, 1201.
22 J. S. Guthi, S. G. Yang, G. Huang, S. Li, C. Khemtong, C. W. Kessinger, M. Peyton, J. D. Minna, K. C. Brown and J. Gao, *Mol. Pharmaceutics*, 2010, **7**, 32.
23 H. Sun, B. Guo, X. Li, R. Cheng, F. Meng, H. Liu and Z. Zhong, *Biomacromolecules*, 2010, **11**, 848.
24 A. W. York, F. Huang and C. L. McCormick, *Biomacromolecules*, 2010, **11**, 505.
25 A. W. York, S. E. Kirkland and C. L. McCormick, *Adv. Drug Delivery Rev.*, 2008, **60**, 1018.
26 A. E. Smith, X. Xu and C. L. McCormick, *Prog. Polym. Sci.*, 2009, **55**, 45.
27 C. Boyer-Kowollik, V. Bulmus, T. P. Davis, V. Ladmiral, J. Liu and S. Perrier, *Chem. Rev.*, 2009, **109**, 5402.
28 C. Barner-Kowollik and S. Perrier, *J. Polym. Sci., Part A: Polym. Chem.*, 2008, **46**, 5715.
29 D. Chen, N. Li, H. Gu, X. Xia, Q. Xu, J. Ge, J. Lu and Y. Li, *Chem. Commun.*, 2010, **46**, 6708.
30 Y. Mitsukami, M. S. Donovan, A. B. Lowe and C. L. McCormick, *Macromolecules*, 2001, **34**, 2248.
31 B. R. Kaafarani, B. Wex, F. Wang, O. Catanescu, L. C. Chien and D. C. Neckers, *J. Org. Chem.*, 2003, **68**, 5377.
32 S. Perrier, P. Takolpuckdee and C. A. Mars, *Macromolecules*, 2005, **38**, 2033.
33 S. Dhar, Z. Liu, J. Thomale, H. Dai and S. J. Lippard, *J. Am. Chem. Soc.*, 2008, **130**, 11467.
34 J. Park, K. An, Y. Hwang, J. G. Park, H. J. Noh, J. Y. Kim, J. H. Park, N. M. Hwang and T. Hyeon, *Nat. Mater.*, 2004, **3**, 891.
35 E. S. Lee, K. T. Oh, D. Kim, Y. S. Youn and Y. H. Bae, *J. Controlled Release*, 2007, **123**, 19.
36 C. Yan, J. K. Kepa, D. Siegel, I. J. Stratford and D. Ross, *Mol. Pharmacol.*, 2008, **74**, 1657.
37 J. Rao, Z. Luo, Z. Ge, H. Liu and S. Liu, *Biomacromolecules*, 2007, **8**, 3871.
38 A. Ramakrishnan and R. Dhamodharan, *Macromolecules*, 2003, **36**, 1039.
39 J. Sudimack and R. J. Lee, *Adv. Drug Delivery Rev.*, 2000, **41**, 147.
40 H. Yuan, K. Luo, Y. Lai, Y. Pu, B. He, G. Wang, Y. Wu and Z. Gu, *Mol. Pharmaceutics*, 2010, **7**, 953.

41 T. K. Jain, M. A. Morales, S. K. Sahoo and D. L. Leslie, *Mol. Pharmaceutics*, 2005, **2**, 194.
42 X. Yang, S. Pilla, J. J. Grailer, D. A. Steeber, S. Gong, Y. Chen and G. Chen, *J. Mater. Chem.*, 2009, **19**, 5812.
43 S. Laurent, D. Forge, M. Port, A. Roch, C. Robic, L. V. Elst and R. N. Muller, *Chem. Rev.*, 2008, **108**, 2064.
44 J. M. Perez, L. Josephson, T. O'Loughlin, D. Högemann and R. Weissleder, *Nat. Biotechnol.*, 2002, **20**, 816.
45 J. M. Perez, T. O'Loughlin, F. J. Simeone, R. Weissleder and L. Josephson, *J. Am. Chem. Soc.*, 2002, **124**, 2856.
46 L. Josephson, J. M. Perez and R. Weissleder, *Angew. Chem., Int. Ed.*, 2001, **40**, 3204.



 